

# Effects of finite curvature on soliton dynamics in nonlinear Schrödinger models

Peter L. Christiansen,<sup>a,★</sup> Yuri B. Gaididei,<sup>b</sup>  
Serge F. Mingaleev<sup>b</sup>

<sup>a</sup>*Department of Mathematical Modelling, The Technical University of Denmark,  
DK-2800 Lyngby, Denmark*

<sup>b</sup>*Bogolyubov Institute for Theoretical Physics, 03143 Kiev, Ukraine*

---

## Abstract

For a curved chain of nonlinear oscillators it is shown that the interplay of curvature and nonlinearity may lead to symmetry breaking when an asymmetric stationary state becomes energetically more favorable than a symmetric stationary state. This phenomenon is studied analytically for a minimal model which effectively takes into account both mechanisms of localization: linear and nonlinear ones. It is shown that the energy of localized states decreases with increasing curvature, i.e. a bend is a trap for nonlinear excitations. The scattering process, i.e. transmission and reflection of moving nonlinear excitations in their passage through the bend is also investigated.

*Key words:* Nonlinear excitations; Curvature; Long-range interaction; Symmetry breaking; Scattering.

---

## 1 Introduction

Recently, determination of the dynamical properties of physical systems with nontrivial geometry has attracted a growing interest because of their wide applicability in various physical and biophysical problems. Examples are biological macromolecules, nanotubes, microtubules, vesicles, electronic and photonic wave-guide structures [1–6]; the gene transcription is usually accompanied by a local DNA bending [7–9]; the electronic properties of carbon nanotubes drastically depend on their chirality [10]; T-shape junctions were recently

---

★ Corresponding author. E-mail: plc@imm.dtu.dk

proposed [11] as nanoscale metal-semiconductor-metal contact devices; periodically spaced, curved optical waveguides were proposed for observation of optical Bloch oscillations [12].

It is well known that the geometry manifests itself in the creation of linear quasi-bound states (see e.g. [13,14]). On the other hand, it is also very well known that the balance between nonlinearity and dispersion provides an existence of spatially localized low-energy soliton-like excitations. Taken together these two localization mechanisms compete and one may expect that the *interplay of geometry and nonlinearity can lead to qualitatively new effects*.

Classical Heisenberg model on an infinite elastic cylinder was considered in [15]. It was shown that a periodic topological spin soliton induces a periodic pinch of the cylindrical manifold [16]. These results are applicable to microtubules and vesicles comprised of magnetic organic materials [17]. The stationary lasing of the modes in a microdisk was investigated in [18]. It was shown that nonlinear whispering gallery modes exist in the microdisk above finite pumping thresholds.

The basic dynamics of deep water and plasma waves, light pulses in nonlinear optics and charge and energy transport in condensed matter and biophysics is described by the fundamental nonlinear Schrödinger (NLS) equation,  $i\partial_t\psi + \partial_x^2\psi + f(x, |\psi|^2)\psi = 0$ , where the function  $f(x, |\psi|^2)$  characterizes the nonlinearity of the medium, e.g. self-interaction of the quasi-particles in the condensed system. The complete integrability of this equation for  $f(x, |\psi|^2) = |\psi|^2$  was established in the seminal paper [19]. Soliton-like excitations of near-integrable NLS systems are very robust and propagate without significant energy loss. Their collisions are almost elastic.

In this paper we consider nonlinear Schrödinger (NLS) models on a curved one-dimensional manifold and investigate how the competition between curvature and nonlinearity affects the nonlinear excitations of the system. The paper is organized as follows. In Sec. II we describe the discrete NLS model on a curved chain and present the results of numerical simulations of stationary states. We discuss the multistability phenomenon and curvature-induced symmetry breaking for non-topological solitary excitations. In Sec. III we present a minimal model which gives qualitatively the same behavior as the original model. In Sec. IV we consider dynamical properties of nonlinear excitations in the curved NLS chain. Section V presents the concluding discussion.

## 2 System and equations of motion

The model we study is described by the Hamiltonian

$$H = - \sum_n \left\{ \sum_{m \neq n} J_{n,m} \psi_n^* \psi_m + \frac{1}{2} |\psi_n|^4 \right\} , \quad (1)$$

where  $\psi_n(t)$  is the complex amplitude at the site  $n$  ( $n = 0, \pm 1, \pm 2, \dots$ ). For instance in the case of the two-strand DNA model [21],  $\psi$  is the complex amplitude of the base-pair stretching vibration. The excitation transfer  $J_{n,m}$  in the dispersive term depends on the distance in the embedding space between the sites  $n$  and  $m$ :  $J_{n,m} \equiv J(|\vec{r}_n - \vec{r}_m|)$ , where the radius-vector  $\vec{r}_n = (x_n, y_n, z_n)$  characterizes the position of the site  $n$  on the manifold. Of course when  $J_{n,m}$  models electromagnetic coupling between dipoles this coefficient will depend also on the relative angles. However, in some cases this dependence is not present. E.g., when the dipoles are orthogonal to the plane in which the chain is located, the corresponding interaction depends only on the distance between the dipoles.

From the Hamiltonian (1) we obtain the equation of motion in the form

$$i \frac{d}{dt} \psi_n + \sum_m J_{n,m} \psi_m + |\psi_n|^2 \psi_n = 0 . \quad (2)$$

The Hamiltonian  $H$  and the number of excitations (quanta)  $N = \sum_n |\psi_n|^2$  are both conserved quantities. The sites are assumed to be equidistantly placed on a plane envelope curve. We consider the properties of nonlinear excitations in the vicinity of smooth bends where the envelope curve without loss of generality can be modelled by a parabola (see the top part of Fig. 3):  $y_n = \kappa x_n^2/2$  and  $z_n = 0$  with  $\kappa$  being the inverse radius of curvature at the bending point. The distance between neighboring sites is assumed to be independent on the curvature  $\kappa$ :  $|\vec{r}_{n+1} - \vec{r}_n| = 1$ . Therefore, when  $\kappa$  is not too big ( $|\vec{r}_m - \vec{r}_n| > 1$  for all  $|n - m| > 1$ ) the excitation dynamics does not depend on the curvature of the system in the *nearest-neighbor approximation*, when  $J_{n,m} = J\delta_{n-m, \pm 1}$ . In many physical problems, however, the nearest-neighbor approximation is too crude. For example, the DNA molecule contains charged groups, and therefore the vibration-excitation transfer is due to the dipole-dipole interaction decaying with the distance  $r$  as  $1/r^3$ . Effective dispersive interaction between nonlinear layers in nonlinear dielectric superlattices is exponential,  $\exp(-\alpha r)$ , with the inverse radius  $\alpha$  depending on parameters of the lattice (superlattice spacing, linear refractive index and so on) [20]. We have investigated both cases,  $J_{n,m} = J \exp(-\alpha |\vec{r}_n - \vec{r}_m|)$  and  $J_{n,m} = J |\vec{r}_n - \vec{r}_m|^{-s}$ , with qualitatively the same results. In this paper, however, we discuss only the first case in detail. It is known [22] that in the case of straight line ( $\kappa = 0$ ) such NLS model exhibits (for  $\alpha < 1.7$ ) bistability in the spectrum of nonlinear stationary states. To distinguish these effects from the finite curvature effects we use  $\alpha = 2$  in what follows.

Early in the game we study stationary states of the system  $\psi_n(t) = \phi_n(\Lambda) e^{i\Lambda t}$ , where  $\Lambda$  is the nonlinear frequency and  $\phi_n(\Lambda)$  is the amplitude in the  $n$ -th site. Figure 1 shows  $N$  versus  $\Lambda$  obtained numerically for the straight chain and curved chain. As may be inferred from this figure, several new features arise as a consequence of the finite curvature:

- *There is a gap* at small  $\Lambda$  in which no localized solution can exist. The gap originates from the existence, in the linear case, of a localized mode with two humps created by the curvature. The gap increases when the curvature  $\kappa$  increases.
- There are *two branches of stationary states*: a branch of symmetric localized excitations (s), which exists for all values of  $N$ , and a branch of *asymmetric localized excitations* (as), which exists only for  $N > N_{th}(\kappa)$ . The threshold value  $N_{th}(\kappa)$  decreases when  $\kappa$  decreases and vanishes in the limit  $\kappa \rightarrow 0$ . The symmetric stationary state has a two-humped shape (evolved from the linear two-hump localized mode) while in the asymmetric state the maximum is shifted either to the left or to the right from the center of symmetry  $n = 0$  (see inset in Fig. 1).
- For the symmetric stationary states  $N(\Lambda)$  is *non-monotonic* as in Refs. [22,23] for NLS models on the straight chain with the radius of the dispersive interaction ( $\sim 1/\alpha$ ) above a critical value. Similarly, in the case of curved chain there is an interval of  $N$  in which three different symmetric states coexist for each excitation number. Taking into account that for the inverse radius  $\alpha = 2$  under investigation there is no bistability in the straight chain (see dot-dashed line in Fig. 1), one may conclude that *bistability is facilitated in the systems with finite curvature*.

The energy of the symmetric as well as asymmetric localized states is monotonically decreasing function of the curvature (see Fig. 2). Thus, one may expect that the *nonlinear localized excitation may facilitate bending of flexible molecular chain*. For  $N > N_{th}(\kappa)$ , when symmetric and asymmetric stationary states coexist, the *asymmetric state is always energetically more favorable*. Taking into account that in the linear limit the ground state of the model is symmetric with respect to the center of symmetry  $n = 0$  one can conclude that *combined action of the finite curvature and nonlinearity provides the symmetry breaking* in the system.

Apart from the smooth bending we studied the case of the wedge:  $y_n = |x_n| \tan(\theta)$ , and obtained qualitatively the same results. We checked also that the exact form of the dispersive interaction is not of serious concern here. To this end we studied the case when the dispersive interaction has the power dependence on the distance:  $J_{n,m} = J|\vec{r}_n - \vec{r}_m|^{-s}$ . Qualitatively the same results were obtained for this case, too. The symmetry breaking, which we observe, means that there is a bistability in the spectrum of nonlinear excitations: the excitation can be localized either at the LHS or the RHS of the bending point

of the chain. By applying an external periodic field one can achieve switching between these two states. In this way we may expect a new resonance to appear in the response of the system to periodic driving.

### 3 Analytical approach and minimal model

Now we turn to discussing the continuum limit of the discrete NLS model given by Eqs. (1)–(2). We are interested here in the case when the characteristic size of the excitation is much larger than the lattice spacing. It permits us to replace  $\psi_n(t)$  by the function  $\psi(\ell, t)$  of the arclength  $\ell$  which is the continuum analogue of  $n$ . Using the Euler-Mclaurin summation formula [24] we get

$$H = \int_{-\infty}^{\infty} \left\{ \frac{1}{2m(\ell)} \left| \frac{\partial \psi}{\partial \ell} \right|^2 + U(\ell) |\psi|^2 - \frac{1}{2} |\psi|^4 \right\} d\ell. \quad (3)$$

Here  $m^{-1}(\ell) = \int_{-\infty}^{\infty} (\ell' - \ell)^2 J_{\ell, \ell'} d\ell'$  is the inverse effective mass of the excitation, and  $U(\ell) = - \int_{-\infty}^{\infty} J_{\ell, \ell'} d\ell'$  is the energy shift due to the dispersive interaction. Near the bending point the number of neighbors available for excitation is larger than far away where the curvature is small. Near the bending the effective potential,  $U(\ell)$ , exhibits a double-well shape. This fact together with the resulting double-well spatial dependence of the effective mass,  $m(\ell)$ , are the reasons why the excitation is localized. The attractive potential  $U(\ell)$  consists of two symmetric wells whose positions ( $\pm a$ ) and depths ( $\Delta \equiv U(|\ell| \rightarrow \infty) - U(a)$ ) are determined by the range of the dispersive interaction and the peculiarities of the bending geometry (see Fig. 3). E.g., in the case of the wedge,  $y_n = |x_n| \tan(\theta)$ , we get for  $\theta < \pi/4$

$$U(\ell) = -\frac{J}{\alpha} (2 - e^{-\alpha|\ell|}) - \frac{J}{\alpha} \begin{cases} e^{-\alpha|\ell| \cos(2\theta)} & \text{when } \theta < 1/2, \\ \alpha |\ell| K_1(\alpha|\ell|) & \text{when } \theta \rightarrow \pi/4, \end{cases}$$

where  $K_n(z)$  denotes the modified Bessel function [24]. The distance between the potential minima  $2a \approx (1 + \theta^2)/\alpha$  and their depth  $\Delta \approx 4eJ\theta^2/\alpha$  increase when the wedge angle  $\theta \rightarrow \pi/4$ . Note that the Hamiltonian similar to Eq. (3) with  $U(\ell) \equiv 0$  was introduced in Ref. [25] to study the effects of the DNA bending on breather trapping. The step function dependence of the effective mass  $m(\ell)$  was there assumed.

The NLS model (3) is still very difficult to solve analytically. But it is interesting anyway to find a model — chosen as simple as possible — which

gives qualitatively the same results as the original model. Such a model can be obtained by using step-wise approximation

$$U(\ell) = -\frac{2J}{\alpha} - \Delta \sum_{\sigma=\pm} (H(\ell - \sigma a + w/2) - H(\ell - \sigma a - w/2)) , \quad (4)$$

where  $H(x)$  is the Heaviside step-function,  $w$  is the width of the potential well. The similar expression can be written for the effective mass  $m(\ell)$ . In the step-wise approach the stationary equation which corresponds to the Hamiltonian (3) can be solved and the corresponding eigenvalue problem can be explored. However, results obtained in this manner look very cumbersome. Therefore we shall make a further simplification by applying the limit  $w \rightarrow 0$ , keeping the product  $w \Delta \equiv \epsilon$  constant in Eq. (4). In this way we arrive at the following minimal model

$$i \frac{\partial \psi}{\partial t} + \frac{\partial^2 \psi}{\partial \ell^2} + \epsilon(\delta(\ell - a) + \delta(\ell + a))\psi + |\psi|^2\psi = 0 , \quad (5)$$

where the gauge-transformation  $\psi \rightarrow \psi \exp(-i2Jt/\alpha)$  was used. Introducing into Eq. (5) the stationary state ansatz  $\psi(\ell, t) = \phi(\ell) \exp(i\Lambda t)$  where  $\phi(\ell) \rightarrow 0$  when  $|\ell| \rightarrow \infty$ , we find that

$$\phi(\ell) = \begin{cases} \sqrt{2\Lambda} \operatorname{sech}(\sqrt{\Lambda}(\ell - \ell_{-1})) & \text{when } \ell < -a, \\ \sqrt{\frac{2\Lambda(1-m)}{2-m}} \operatorname{nd}\left(\sqrt{\frac{\Lambda}{2-m}}(\ell - \ell_0) \mid m\right) & \text{when } |\ell| < a, \\ \sqrt{2\Lambda} \operatorname{sech}(\sqrt{\Lambda}(\ell - \ell_1)) & \text{when } \ell > a \end{cases}$$

where  $\operatorname{pq}(u \mid m)$  ( $p, q = c, s, d, n$ ) are the Jacobi elliptic functions with the modulus  $m$  [24]. The parameters  $\ell_{\pm 1}, \ell_0$ , and  $m$  are determined from the relations

$$\begin{aligned} \operatorname{sech}(\sqrt{\Lambda}(a \mp \ell_{\pm 1})) &= \sqrt{\frac{1-m}{2-m}} \operatorname{nd}\left(\sqrt{\frac{\Lambda}{2-m}}(a \mp \ell_0 \mid m)\right), \\ F(\ell_0, m) &\equiv \sqrt{1-m(1-m)} \operatorname{sd}^2(u_+ \mid m) + m \operatorname{sd}(u_+ \mid m) \operatorname{cn}(u_+ \mid m) - \\ &\quad \sqrt{1-m(1-m)} \operatorname{sd}^2(u_- \mid m) + m \operatorname{sd}(u_- \mid m) \operatorname{cn}(u_- \mid m) = 0, \\ \sqrt{1-m(1-m)} \operatorname{sd}^2(u_{\pm} \mid m) + m \operatorname{sd}(u_{\pm} \mid m) \operatorname{cn}(u_{\pm} \mid m) &= \sqrt{\frac{2-m}{\Lambda}} \epsilon, \end{aligned} \quad (6)$$

where  $u_{\pm} = \sqrt{\Lambda/(2-m)}(a \pm \ell_0)$ . Using the above expressions one can evaluate the number of excitations which corresponds to the stationary solution

$$N = 4(\sqrt{\Lambda} - \epsilon) + 2\sqrt{\frac{\Lambda}{2-m}} \sum_{\sigma=\pm 1} E(\text{am}(u_\sigma) | m) \quad (7)$$

where  $\text{am}(u)$  is the amplitude and  $E(\phi | m)$  is the elliptic integral of the second kind [24].

The equation  $F(\ell_0, m) = 0$  always has a solution  $\ell_0 = 0$ . This corresponds to the symmetric two-hump wave function  $\phi(\ell)$ . In addition,  $\ell_0 \neq 0$  solutions appear for  $\Lambda \geq \Lambda_c$  with the threshold value  $\Lambda_c$  being determined from the condition  $\partial F / \partial \ell_0 = 0$  for  $\ell_0 = 0$ . In other words, a symmetry-breaking bifurcation to a doubly degenerate branch of asymmetric solutions occurs in the point  $\Lambda = \Lambda_c$ . It follows from Eq. (6) that the symmetry-breaking bifurcation is determined by the equation  $(1 - 2\text{sn}^2 + m\text{sn}^4) \sqrt{1 - 2m\text{sn}^2 + m^2\text{sn}^2} = (1 - m) \text{sn} \text{cn}$  with  $\text{sn} \equiv \text{sn}(\sqrt{\Lambda/(2-m)} | m)$ .

The results of the analytical consideration of the nonlinear eigenvalue problem based on Eqs. (6) and (7) are shown in Fig. 4. As in the original model the stationary state (s) is unique and symmetric for small number of quanta  $N$ . But when the number of quanta exceeds some critical value there are two stationary states: symmetric (s) and asymmetric (as), with the asymmetric state being energetically favorable. Thus, similarly to the original model, the minimal model demonstrates a symmetry breaking effect (localization in one of the wells).

## 4 Dynamical properties of excitations

### A. Standing excitations

The stability of immobile stationary excitations in the curved chain of nonlinear oscillators was investigated in [26]. It was shown that the symmetric two-humped stationary state possesses two localized internal modes: Peierls antisymmetric mode i.e. the mode which is responsible for the center of mass motion, and breathing symmetric mode. There are two intervals of instability of the symmetric stationary state: when  $\Lambda_1(\kappa) < \Lambda < \Lambda_2(\kappa)$  the stationary state is unstable with respect to the Peierls mode and when  $\Lambda_2(\kappa) < \Lambda < \Lambda_3(\kappa)$  it is unstable with respect to the breathing mode.

A typical evolution of the symmetric stationary state in the case when it becomes unstable with respect to the Peierls mode is shown in Fig. 5. One can see that the two-humped initial symmetric state evolves into an asymmetric state with an excited breathing internal mode.

### B. Moving excitations

We also investigated the scattering of moving excitations in their passage through the center of the parabolic chain  $y_n = \kappa x_n^2/2$ . We obtained the stationary moving excitations required for this purpose by pushing of initially unmoving stationary states  $\phi_n$  found numerically in Sec. II far away from the center of the chain ( $\psi_n(0) = \phi_n(\Lambda) e^{ikn}$  with some  $k$  and  $\Lambda$ ). Eventually, evolving over the course of 5000 time units, the excitation reached almost stationary form and velocity  $v$  as the center of the chain was approached (e.g.,  $N = 2.39$  and  $v = 0.37$  in Figs. 6–10 discussed below). But the destiny of the excitation in passing through the center turned out to be strongly dependent on the curvature of the chain  $\kappa$ . In Fig. 6 we plot the velocity  $v_{sc}$  of the moving part of the excitation after the passage of the bent region versus the curvature  $\kappa$ . One can distinguish four different regimes:

- For small  $\kappa$  ( $\kappa < 0.2$ ) the bending practically does not influence the excitation motion. Inelastic transmission takes place when  $0.2 < \kappa < 1.07$ . The excitation passes the bent region leaving behind a part of its energy in the form of linear localized mode (see Fig. 7).
- In the interval  $1.07 < \kappa < 2.1$  the excitation is captured by the bend (see Fig. 8).
- When  $2.1 < \kappa < 2.6$  the excitation reflects from the bend but the significant part of the initial energy of the excitation is trapped at the bending region (see Fig. 9).
- When  $\kappa > 2.6$  the main part of the excitation energy reflects from the bend while the rest is captured by the bend (see Fig. 10).

## 5 Conclusions

In conclusion, we have shown that in the NLS model on the curved one-dimensional manifold the interplay of curvature and nonlinearity leads to the symmetry breaking, when the asymmetric stationary state becomes energetically favorable than the symmetric one. We have found that the energy of localized states decreases with the increasing of curvature. We expect that the nonlinear localized excitation may facilitate bending of a flexible molecular chain. In all cases bending manifests itself as a trap for nonlinear excitations. Qualitatively the same properties are found in the case of the physically important dipole-dipole dispersive interaction  $J_{nm} = |\vec{r}_n - \vec{r}_m|^{-3}$ . Specifically, in the case of the Davydov-Scott model [27,28] with the dipole-dipole coupling between sites [29] for the parameters which characterize the motion of the amide-I excitation in proteins (they correspond to  $N = 0.64$  in our model) decreasing of the ground state energy due to a trapping by the bending with



$\kappa = 1$  ( $\kappa = 3$ ) comprise 10% (46%) of the whole excitation energy. This may be also important for the dynamics of DNA molecule where as was mentioned above the vibration-excitations are described by Eq. (2) with the dipole-dipole dispersive interaction [30].

## Acknowledgments

We thank A.C. Scott for the helpful discussions. Yu.B.G. and S.F.M. would like to express their thanks to the Department of Mathematical Modelling, Technical University of Denmark where the major part of this work was done. S.F.M. acknowledges support from the Australian Research Council.

## References

- [1] W. Saenger, *Principles of Nuclear Acid Structure* (Springer-Verlag, Berlin, 1984).
- [2] S. Iijima, *Nature* **354**, 56 (1991).
- [3] R. Bar-Ziv and E. Moses, *Phys. Rev. Lett.* **73**, 1392 (1994); P. Nelson, T. Powers, and U. Seifert, *ibid.* **74**, 3384 (1995).
- [4] *Physics of Amphiphilic Layers*, Eds.: J. Meunier, D. Langevin, and N. Boccaro (Springer-Verlag, Berlin, 1987).
- [5] Y. Imry, *Introduction to Mesoscopic Physics*, (Oxford University Press, New York, 1997).
- [6] *Photonic Band Gaps and Localization*, Ed.: C. M. Soukoulis (Plenum Press, New York, 1993).
- [7] C. Reiss, in *Nonlinear Excitations in Biomolecules*, Ed.: M. Peyrard (Springer, Berlin, Les Editions de Physique, Les Ullis, 1995), p. 29.
- [8] H. Heumann, M. Ricchetti, and W. Werel, *EMBO J.* **7**, 4379 (1988).
- [9] S. K. Burley, *Nature Struct. Biology* **1**, 638 (1994); J. L. Kim, D. B. Nikolov, and S. K. Burley, *Nature* **365**, 520 (1993).
- [10] N. Hamada, S. Sawada, and A. Oshiyama, *Phys. Rev. Lett.* **68**, 1579 (1992).
- [11] M. Menon and D. Srivastava, *Phys. Rev. Lett.* **79**, 4453 (1997).
- [12] G. Lenz, I. Talanina and C. M. de Sterke, *Phys. Rev. Lett.* **83**, 963 (1999).
- [13] G. Kirczenow, *Phys. Rev. B* **39**, 10452 (1989).

- [14] Yu. B. Gaididei, L. I. Malysheva, and A. I. Onipko, *Journ. Phys.-Cond. Matt.* **4**, 7103 (1992).
- [15] R. Dandoloff, S. Villain-Guillot, A. Saxena, and A. R. Bishop, *Phys. Rev. Lett.* **74**, 813 (1995); A. Saxena and R. Dandoloff, *Phys. Rev. B* **55**, 11049 (1997).
- [16] A manifold is a geometric object which locally has the structure of  $\mathcal{R}^3$  or some other vector space. This fundamental idea refines and generalizes, to an arbitrary dimension, the notions of a line or a surface.
- [17] A. Saxena, R. Dandoloff, T. Lookman, *Physica A* **261**, 13 (1998).
- [18] T. Harayama, P. Davis, K. S. Ikeda, *Phys. Rev. Lett.* **82**, 3803 (1999).
- [19] V. E. Zakharov and A. B. Shabat, *Sov. Phys. JETP*, **34**, 62 (1972).
- [20] Yu. B. Gaididei, P. L. Christiansen, K. Ø. Rasmussen, and M. Johansson, *Phys. Rev. B* **55**, R13365 (1997).
- [21] Yu. B. Gaididei, S. F. Mingaleev, P. L. Christiansen, M. Johansson, and K. Ø. Rasmussen, in *Adriatico Research Conference (1997: Trieste, Italy) Nonlinear Cooperative Phenomena in Biological Systems*, Ed.: Leif Mattson (World Scientific, Singapore 1998), p. 176.
- [22] M. Johansson, Yu. B. Gaididei, P. L. Christiansen, and K. Ø. Rasmussen, *Phys. Rev. E* **57**, 4739 (1998).
- [23] Yu. B. Gaididei, S. F. Mingaleev, P. L. Christiansen, and K. Ø. Rasmussen, *Phys. Rev. E* **55**, 6141 (1997).
- [24] M. Abramowitz and I. Stegun, *Handbook of Mathematical Functions* (Dover Publications, Inc., New York, 1972).
- [25] J. J.-L. Ting and M. Peyrard, *Phys. Rev. E* **53**, 1011 (1996).
- [26] Yu. B. Gaididei, S. F. Mingaleev, and P. L. Christiansen, *Curvature-induced symmetry breaking in nonlinear Schrödinger models*, Los-Alamos preprint *patt-sol/9907003* (1999).
- [27] A.S. Davydov, *Solitons in Molecular Systems* (D.Reidel Publishing Company, Dordrecht-Boston-Lancaster, 1985).
- [28] A. C. Scott, *Phys. Rep.* **217**, 1 (1992).
- [29] L. Cruzeiro-Hansson, *Phys. Lett. A* **249**, 465 (1998).
- [30] S. F. Mingaleev, P. L. Christiansen, Yu. B. Gaididei, M. Johansson, and K. Ø. Rasmussen, *J. Biol. Phys.* **25**, 41 (1999).

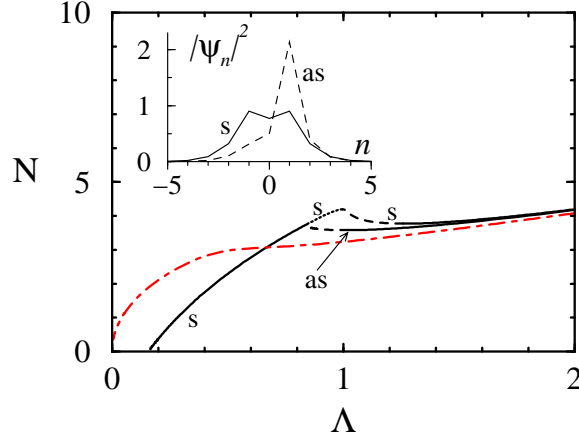


Fig. 1. The number of excitations  $N(\Lambda)$  for the straight chain ( $\kappa = 0$  ; dot-dashed line) and curved chain ( $\kappa = 3$  ; solid, dotted, and dashed lines) for  $\alpha = 2$  and  $J = 6.4$ . In the inset shapes of the symmetric (s) and asymmetric (as) stationary states for  $N = 3.6$  are shown.

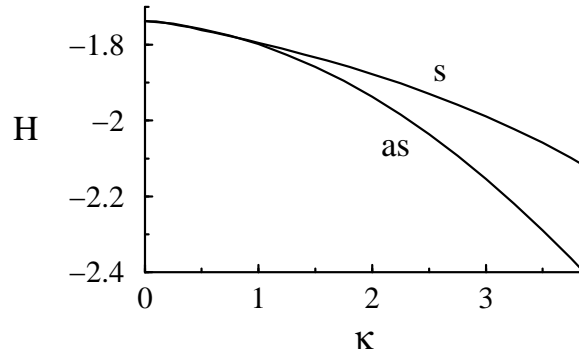


Fig. 2. Energy of symmetric (s) and asymmetric (as) nonlinear excitations versus the curvature  $\kappa$  for  $\alpha = 2$ ,  $J = 6.4$ , and  $N = 4$ .

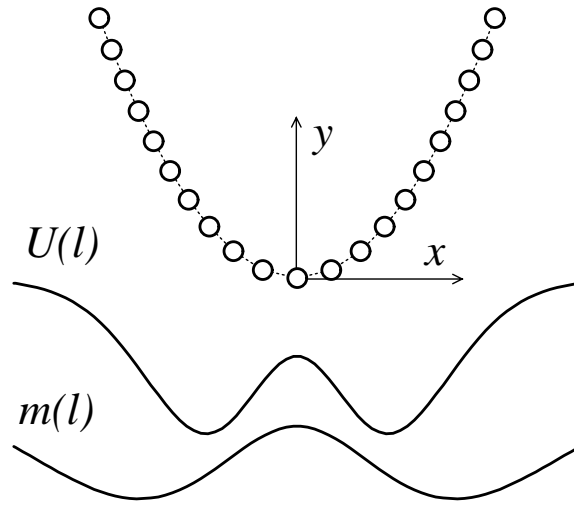


Fig. 3. The curved chain under consideration and the corresponding double-well effective potential  $U$  and mass  $m$ .

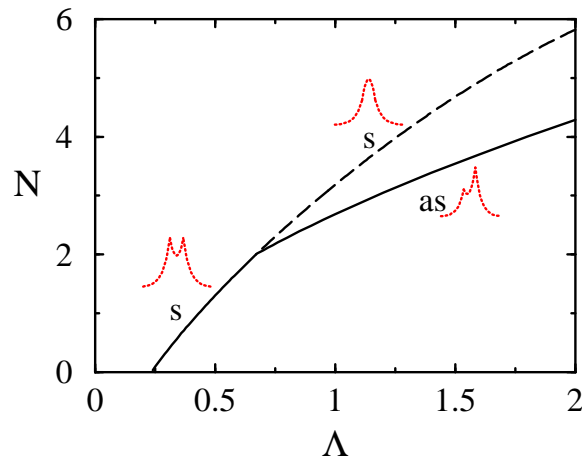


Fig. 4. The dependence  $N(\Lambda)$  for symmetric (s) and asymmetric (as) nonlinear excitations in the two-impurity minimal model (5) with  $\epsilon = 0.7$  and  $a = 1$ .

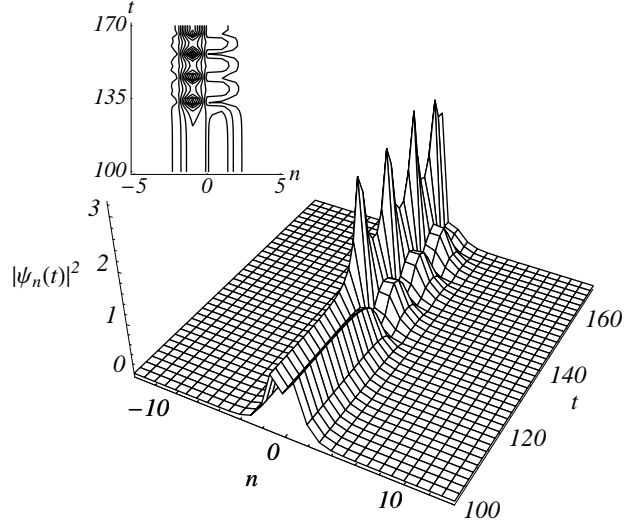


Fig. 5. Switching from the symmetric state to the asymmetric state at  $\alpha = 2$ ,  $J = 6.4$ ,  $\kappa = 4$ , and  $N = 3.96$ .

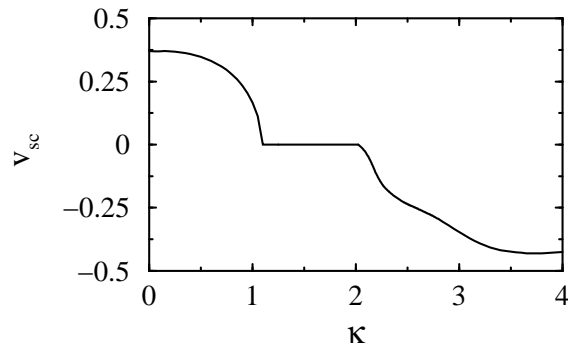


Fig. 6. Velocity  $v_{sc}$  of the moving part of the excitation after the passage of the center of the parabolic chain versus the curvature  $\kappa$ . Here  $\alpha = 2$ ,  $J = 6.4$ ,  $N = 2.39$  and initial velocity  $v = 0.37$ .

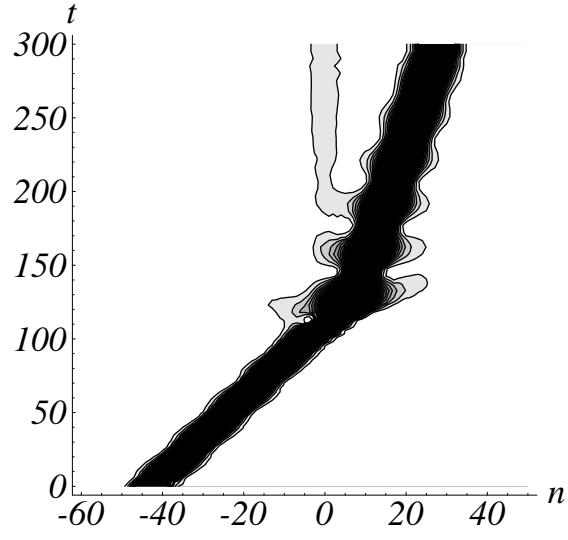


Fig. 7. Density plot of  $|\psi_n(t)|^2$  which demonstrates scattering of the moving excitation for  $\kappa = 1.05$  in Fig. 6.

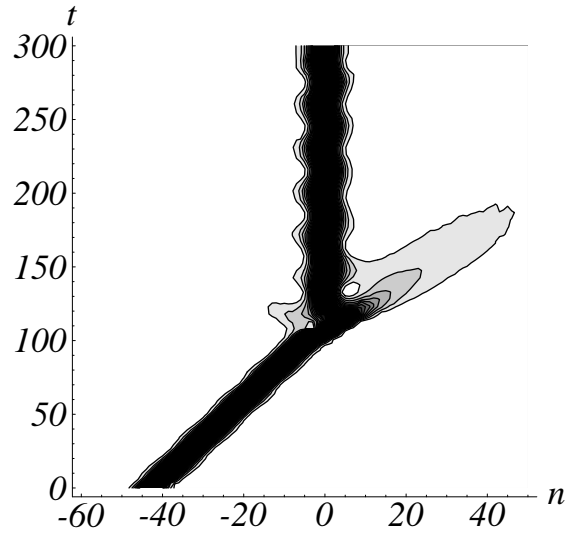


Fig. 8. Density plot of  $|\psi_n(t)|^2$  which demonstrates scattering of the moving excitation for  $\kappa = 1.5$  in Fig. 6.

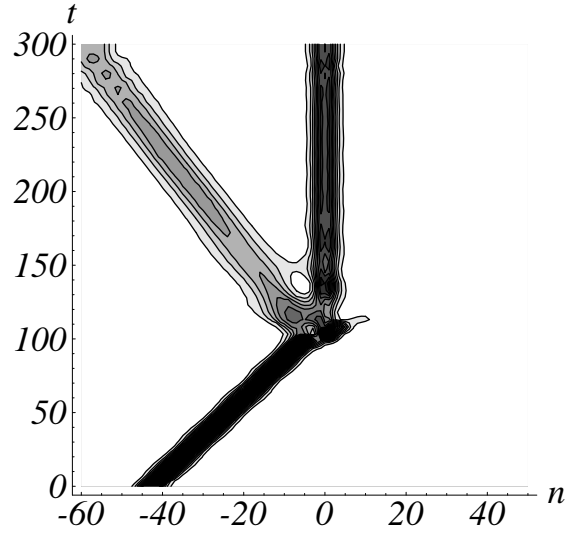


Fig. 9. Density plot of  $|\psi_n(t)|^2$  which demonstrates scattering of the moving excitation for  $\kappa = 2.5$  in Fig. 6.

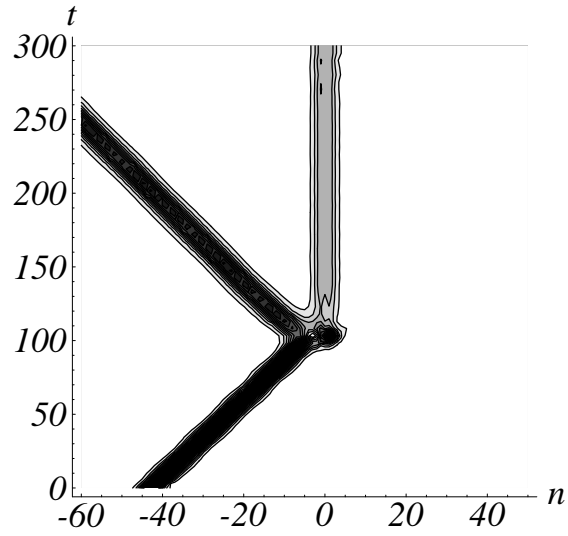


Fig. 10. Density plot of  $|\psi_n(t)|^2$  which demonstrates scattering of the moving excitation for  $\kappa = 3.0$  in Fig. 6.